



Modeling and interactive simulation of measures against infection transmission

Simulation: Transactions of the Society for Modeling and Simulation International
2023, Vol. 99(4) 327–346
© The Author(s) 2022



Article reuse guidelines:
DOI: 10.1177/00375497221133849
journals.sagepub.com/home/sim



Mina Abadeer¹ , Sameh Magharious² and Sergei Gorlatch¹

Abstract

In this paper we develop an approach to modeling and simulating the process of infection transmission among individuals and the effectiveness of protective counter-measures. We base our approach on pedestrian dynamics and we implement it as an extension of the Vadere simulation framework. In order to enable a convenient simulation process for a variety of scenarios, we allow the user to interact with the simulated virtual environment (VE) during run time, for example, by dynamically opening/closing doors for room ventilation and moving/stopping agents for re-positioning their locations. We calibrate and evaluate our approach on a real-life case study—simulating COVID-19 infection transmission in two kinds of scenarios: large-scale (such as the city of Münster, Germany) and small-scale (such as the most common indoor environments—classrooms, restaurants, etc.). By using the tunable parameters of our modeling approach, we can simulate and predict the effectiveness of specific anti-COVID protective measures, such as social distancing, wearing masks, self-isolation, schools closing, etc.

Keywords

Computer simulation, mathematical modeling, multi-agent systems, infection transmission, protective measures, COVID-19, SARS-CoV-2, infection probability

1. Motivation and introduction

When an infectious disease is new, decision-makers (e.g., public health authorities, hospitals, and especially municipalities) try to answer the two most important questions: how does the infection spread, and what measures are necessary and effective to mitigate it? For example, SARS-CoV-2 often starts locally, but it spreads quickly and globally. This makes mitigating the virus very challenging for governments: they must determine the proper guidelines to be applied in time to reduce the spread of the virus.

Unfortunately, lack of reliable data often prevents effective anti-infection measures. The number of people infected is difficult to determine on a daily basis, as symptoms do not occur until a few days after infection. In addition, infection statistics are not available early on in a pandemic, so it is difficult to know how many people have become infected and how many people are already immune to the disease.

Modeling and simulation are useful approaches to answering the questions about the spread of infectious diseases. By adapting the models to a specific infection disease and the conditions of the environment (generally by tunable parameters), the actual situations and

developments can be described and analyzed. Furthermore, computer simulation can offer viable means for hypothesis testing, evaluating best- and worst-case scenarios, and assessing the effect of different measures on outbreaks of disease.

Traditional models for describing the dynamics of disease development divide the population into several categories: Susceptible (S), Exposed (E), Infected (I), and Recovered (R). This leads to four classes of pandemic models: SI, SIS, SIR, and SEIR.^{1,2} A major problem with traditional models, especially for predicting the virus transmission, is that they are static. Usually, they contain fixed values for several parameters, while ignoring other key parameters. Important limitations are for example: (a) the contact duration among individuals is considered constant; (b) social distancing between individuals is neglected; and

¹University of Münster, Münster, Germany

²Dell Technologies, Bothell, WA, USA

Corresponding author:

Mina Abadeer, University of Münster, Einsteinstr. 62, Room 705, Münster D-48149, Germany.

Email: abadeer@uni-muenster.de

(c) the isolation of infected persons is not taken into account: they are viewed as still infectious. These restrictions strongly limit these models' ability to represent real-life pandemic scenarios.

In this paper, we aim at improving the simulation of infection transmission, by developing a modeling and simulation approach based on pedestrian dynamics. The goal of our approach is to be able to model and simulate potential guidelines for dealing with pandemics that can be defined by governments and municipalities.

Our use case in the paper is the COVID-19 pandemic in Germany. In particular, we evaluate our modeling and simulation approach regarding the most important protective measures that restrict contacts between people^{3,4}: (a) closing restaurants, bars, discos, pubs, and similar facilities; (b) social distancing, hygiene rules, and wearing masks; and (c) closing schools, universities, etc.

The practical benefit of our modeling and simulation approach is that it can predict the likelihood of an infected individual transmitting the infection to others in the most common environments (e.g., restaurants), and to elucidate to what degree closing schools, social distancing guidelines, and wearing masks can help to limit the spread of the virus.

We make the following novel contributions in this paper:

1. We introduce the new concept of behaviors, in particular we model the infection transmission behavior in the Susceptible-Infected-Recovered (SIR)-form and we implement it on top of the agent-based Vadere simulation framework.⁵
2. We simulate social distancing, self-isolation, contacts restriction and using masks, and we test the influence of these protective measures in different scenarios.
3. We model infected people's speaking volume and its influence on spreading of viral particles. This allows us to investigate the effectiveness of controlling individuals' speaking behavior (in particular, singing) for limiting virus spread.
4. We substantially improve the level of user interactivity in our simulation environment: we allow the user to change the state of the simulated environment during simulation run time, for example, change room ventilation by opening/closing doors, moving/stopping agents, etc. Thus, we can simulate various scenarios in real time.
5. We extend the interactivity possibilities of the topography creator in the Vadere framework: in particular, we allow the user to add a city map and scale it in the GUI, in order to visualize large-scale scenarios in addition to small-scale scenarios.
6. Our simulation produces three kinds of output for experts and decision makers: (a) the effective

reproduction factor $R_0^{\text{eff}}(t)$ provides information about the usefulness of protective measures and their combinations; (b) the pandemic curve for each scenario visualizes the pandemic situation development; (c) the probability of infection transmission $PR(t)$ helps to find a useful strategy in a particular environment.

We validate and evaluate our approach in extensive experiments on virtual environments (VEs) of different scale: large-scale—city of Münster in Germany in 40 scenarios, and small-scale—offices, classrooms, restaurants, and large buildings (e.g., concert halls) in 60 different scenarios.

In the remainder of the paper, the related work is discussed in the next Section 2. We describe our concept of behaviors in Section 3 where we model the infection transmission and protective measures, and their implementation in the Vadere framework. In Section 4, we introduce and implement simulation interactivity in VEs. In Section 5, we evaluate our approach by running experiments on different SARS-CoV-2 transmission scenarios that confirm the adequacy and precision of the results predicted by simulation as compared with real-life pandemic curves. We summarize our findings in Section 6.

2. Related work

The availability of accurate information early in the development of a pandemic is important for epidemiological modeling, that is, representing the possible interactions between misinformation spread and disease outcomes.⁶⁻⁸ Despite advances in understanding previous pandemics (influenza, SARS, etc.), simulating the spread of the newest SARS-CoV-2 virus remains challenging. In reference,⁹ effective strategies for controlling the spread of misinformation among individuals during an influenza pandemic were proposed in order to reduce communicable disease burdens in future diseases.

However, since the start of the COVID-19 pandemic, the available data has been and are still noisy and uncertain. In addition to limited and unbalanced global data, the reporting standards for new infections have not been standardized yet, resulting in statistical errors, particularly in underdeveloped regions and countries. One of the most important ways to overcome this challenge is to develop sophisticated, user-interactive, adaptable, and simple-to-use simulation models that can accept changes smoothly and with minimal effort.

Mathematical models of airborne disease infection transmission in indoor environments are often based on the classic work of Wells¹⁰ and Riley et al.¹¹ These models have been used to describe the spread of airborne pathogens such as tuberculosis, measles, influenza, H1N1, and

recently SARS-CoV-2.^{12–16} Such models reflect a situation in which one or more infected individuals stay in the same room with other individuals who are susceptible to infection, and predict the probability of a susceptible individual becoming infected. However, these models rely on a few simple assumptions, for example, that virus particles are distributed uniformly in the environment; they also ignore the dynamics of movements between individuals, which has a significant impact on the probability of infection transmission.

Paper¹⁷ improves the Wells-Riley model by introducing a distance proximity to quantify the impact of social distancing on the probability of infection. However, this method does not take into account the location of infected persons, nor does it consider the changing distance between the infected and susceptible persons in the room over time. This prevents the analysis of individuals' dynamic behavior in the room, which has a direct impact on analyzing the effectiveness of in-door protective measures, for example, social distancing.

In another attempt to overcome the previous limitations, the authors in Guo et al.¹⁶ calculate the spatial distribution of infection probability based on a single airflow calculation in a room, taking into account that the locations of infected individuals are statically distributed in the room with different position arrangements. However, this method is unsuitable for scenarios involving crowding in a small space; it also ignores the effect of the most common protective measures, such as the use of masks, which has a direct impact on the probability of infection transmission. The probability of infection is determined by the exposure of a susceptible individual to an infected individual, which is determined by the dynamics of individual movements and proximity to each other in a room.

The mathematical model developed by RAND Corp.¹⁸ combines information from epidemiology, economics, and a qualitative regulatory analysis to assess the effects of various protective measures. However, it ignores the effect of room ventilation and the infected person's speaking volume on the probability of infection transmission. Taking all these influencing factors into account when selecting model parameters remains a challenge for mathematical modeling.¹⁹

Paper²⁰ presents a discrete-event mathematical model that explores how virus transmission occurs in indoor environments. The replication machinery of the SARS-CoV-2 based on Discrete Event Specifications (DEVS) is described in Ayadi et al.²¹ Such models require an additional effort to design a VE with a complex system of rooms and doors—using external tools, for example, Autodesk—and are thus limited to simulating small-scale scenarios. Agent-based simulations allow for considering control-sensitive parameters in order to estimate their effects on infections, in particular on reproduction number, transmission rate, and pandemic control after

implementing certain protective measures. In Gomez et al.,²² a city-scale, agent-based approach simulates the transmission dynamics of SARS-CoV-2 with implemented social distancing to represent this measure's effectiveness in mitigating the spread of the virus. However, no simulations have been conducted to determine how global interventions, environmental factors, and other relevant policies and measures influence the dynamics of the COVID-19 pandemic. Paper²³ reports the effectiveness of isolation, social distancing, and school closures with different levels of compliance, but it does not consider the effectiveness of wearing masks as a globally applied measure and the impact of an infected individual's speaking volume on spreading virus particles in a room. New approaches are developed by governmental bodies to understand the virus behavior and its attack mechanisms, including the use of high-performance computing in CityCOVID by Argonne National Lab²⁴ and the proprietary framework by MITRE Corp.²⁵

We aim at improving the previous approaches as follows. We combine simulation of infection transmission behavior at the city scale and at the small indoor VE scale among individuals. Our approach allows the user to anticipate the effectiveness of various levels of compliance with globally applied protective measures such as social distancing, self-isolation, school closures, wearing masks, and controlling speaking volume. Last but not least, the user can interact with the VE and change the state of interactive elements, such as opening a door in a closed room to allow agents to exit outdoors or ventilating the room, both of which have a direct impact on the probability of at least one individual being infected.

3. Modeling infection transmission behavior and protective measures

We present our approach to modeling the disease spread as an extension of the Vadere simulation framework.⁵ The original Vadere framework models walking behavior of people (agents) using various locomotion models that were calibrated and validated against empirical real-life observations.^{26,27} Dynamic agent behavior is simulated in a 2D plane by means of the topography visualizer for various locomotion models.

A *topography* in our simulation approach is a combination of the following five kinds of simulation elements:

1. *Agents* have circular shapes and move with particular acceleration or slow-down from a source to the target according to a particular locomotion model.
2. *Obstacles* can be drawn by the user as particular geometric shapes; the agents try to avoid them. Obstacles can also be walls of a VE structure, for example, a building.

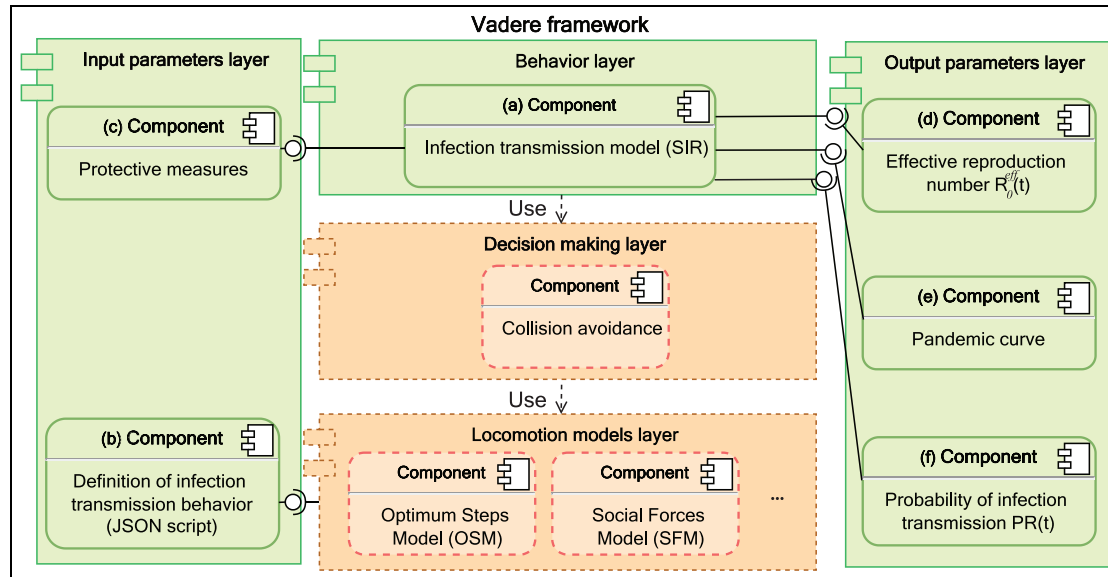


Figure 1. UML component diagram: our infection transmission model on top of the Vadere framework and its parameters.

3. *Sources* are areas in which agents exist individually or in a group. Instead of creating agents in a source area, the user can also position them at a particular place.
4. *Targets* are areas that agents may attempt to reach.
5. *Target changers* are areas where an agent's target is changed if the agent passes through such an area.

Figure 1 shows how we extend the Vadere framework. The original Vadere has two layers (boxes with dashed borders and an orange background) that control the dynamic of agents' movements: the locomotion model layer and the decision making layer. However, they do not provide agents with personal behaviors such as health status (e.g., susceptible, infected, or recovered in pandemics).

In our approach, to simulate the disease spread, we introduce three new layers (boxes with solid borders and a green background): the *behavior layer*, the *input parameters layer*, and the *output parameters layer*. The behavior layer implements a general concept of *agent behavior* which models an individual's behavior, for example, walking, stopping, or infection transmission behaviors. In the behavior layer, we model the infection transmission behavior on top of the locomotion models that control agents' movement.

Each layer contains one or several components. Component (a) implements our infection transmission model that captures the continuous spread of a pandemic in a SIR form.

In the input parameters layer in Figure 1, component (b) provides the model definition in the JavaScript Object Notation (JSON) format²⁸ that allows the behavior to be compatible with the selected locomotion model, which in

this paper is the Optimal Steps Model (OSM),²⁶ as shown in Listing 1.

Listing 1. JSON code definition of infection transmission behavior using OSM model.

```
{
  ``mainModel`` : ``org.vadere.simulator.models.
    osm.OptimalStepsModel``,
  ``attributesModel`` : { ...
  ``org.vadere.state.attributes.models.
    AttributesOSM`` : { ...
  ``behaviors`` : [ ``org.vadere.simulator.
    control.behavior.InfectionBehavior`` ],
    ...
  }
}
```

Component (c) refers to the module of the protective measures that provides the input parameters to our infection model. In the output parameters layer in Figure 1, components (d), (e), and (f) refer to the classes that provide the simulation outputs, namely: the effective reproduction number $R_0^{\text{eff}}(t)$ that is used for assessing the effectiveness of protective measures, the pandemic curve at run time of simulation to visualize the pandemic situation, and the probability of infection transmission $PR(t)$, correspondingly.

Table 1 represents the input parameters of our model; some of them are provided by the user while others (like λ) are pre-computed as explained in subsection 5.3.

Table 1. Input parameters of our infection transmission model.

Parameter	Definition
Agent's radius r_i	radius (physical) of agent i
Infectious radius $r_{i,t+1}$ of agent i at time $t + 1$	infected agent radius used in Equation (1) for computing infection transmission
Infection rate λ	number of infected agents in the environment population pre-computed as in subsection 5.3, used to initialize our model
Average duration of immunity	time during which a recovered agent cannot be infected again
Average duration of infection transmission	time spent by a susceptible agent spent in infectious radius (in min)
Average recovery duration γ	time it takes for infected agent to recover (in days)
Initial infection percentage	percentage of infected agents in the population at simulation start
Physical distance D	distance between the centers of any two agents (in meters)
Duration of contact T	time of contact between two agents
Group size G	number of agents per group
Self-isolation percentage q_{percent}	percentage of infected agents to be isolated until simulation end
Self-isolation start time	time after which the infected agents are self-isolated (in days)
Basic reproduction number R_0	initialized average number of persons who become infected

Table 2. Output parameters of our infection transmission model.

Parameter	Definition
Effective reproduction number $R_0^{\text{eff}}(t)$	number of persons infected by an infectious individual in time t
Probability of infection transmission $PR(t)$	probability that at least one susceptible person becomes infected during contact time t

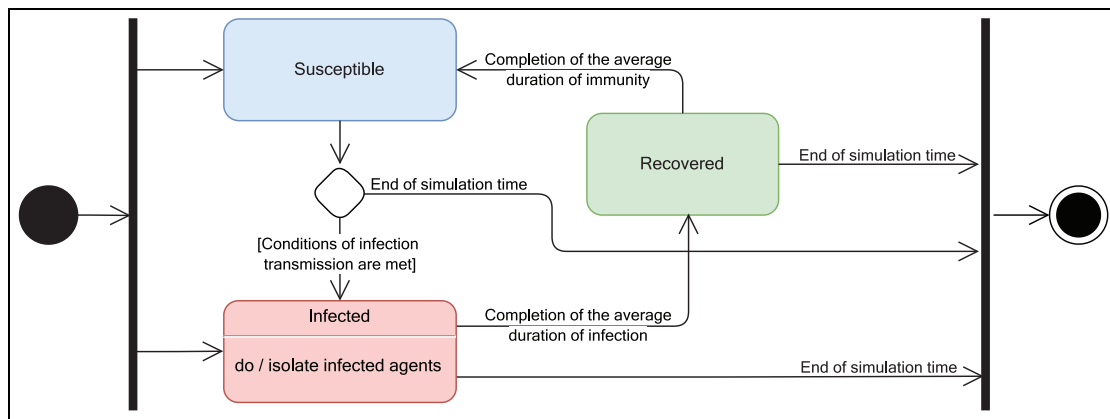


Figure 2. State diagram of our infection transmission model.

Table 2 represents the output parameters of our model; they are computed as the result of simulation.

In the following, we describe our simulation that relies both on the OSM model and Vadere’s decision-making layer responsible for avoiding collisions of agents.

3.1. Modeling infection transmission

Figure 2 shows the state diagram of our infection transmission model: it is of the SIR type. At the first simulation step, the population is divided in two classes—susceptible and infected—based on the parameters (percentages)

defined by the user. At next steps, susceptible agents may become infected if infection transmission conditions are met or they remain susceptible until the end of the simulation. Infected agents can recover and become immune after the average recovery duration. Recovered agents remain immune for the immunity duration (parameter in Table 1). Then their status is changed back to susceptible, and they can become infected again.

In our approach, in each *time step* t , an infected individual i can modify his *infectious radius* $r_{i,t+1}$, according to the *infection rate* λ (explained in subsection 5.3) and to the individual protective measures such as wearing a

mask, controlling one's speaking volume, and following the social distancing guidelines, as described in the next subsection.

Whenever a susceptible agent (S) has contact with an infected agent (I) for an average duration of time T (such as talking to each other) or remains within the agent's infectious radius without direct contact for a time interval τ , the probability of the susceptible agent (S) changing his status to infected (I) increases as defined by Equations 5 and 6.

The infectious radius $r_{i,t+1}$ is computed as follows:

$$r_{i,t+1} = r_i + V/M, \quad (1)$$

where V is the speaking volume: when the speaking volume increases, the virus particles spread for longer distances, resulting in an increase in the infectious radius. M is the mask type: the higher a mask's protection level, the shorter the distance virus particles can spread. V and M are discussed in more detail in the next subsection.

Additionally, the status of an infected agent (I) can be changed to recovered (R) after this agent either (a) spends the *average duration of recovery time* γ and remains immune until the end of simulation (in this paper, $\gamma = 14$ days), or (b) is removed from the simulation by the user. When the status of an agent changes to recovered (R), the agent becomes immune for the immunity duration.

Listing 2 shows the definition of infection transmission behavior and its attributes expressed in the JSON format.

Listing 2. JSON code of the infection transmission behavior.

```
{
  ``mainModel`` : ``org.vadere.simulator.models.
    osm.OptimalStepsModel``,
  ``attributesModel`` : { ...
  ``org.vadere.state.attributes.models.
    AttributesOSM`` : { ...
  ``behaviors`` : [ ``org.vadere.simulator.
    control.behavior.InfectionBehavior`` ]
  },
  ``org.vadere.state.attributes.models.
    infection.AttributesInfectionBehavior``
  : {
  ``minInfectionDistance`` : 0.0,
  ``immunityDurationInDays`` : 30,
  ``durationToTransmitInSteps`` : 1,
  ``recoveryDurationInDays`` : 14,
  ``infectionPercentage`` : 5.0
  ``selfisolationStartTimeInDays`` : 3,
  ``selfIsolationPercentage`` : 20
  }, ...
  }
}
```

Table 3. Parameters of social distancing: risk levels.

Parameter	Social distancing risk levels		
	High	Medium	Low
D (meters)	0.5–1	1.1–2	2.1–3
T (min)	15	5	2
G (members/group)	5	3	–

3.2. Modeling protective measures

In the following, we explain how we model three kinds of protective measures: social distancing, self-isolation, and wearing a mask of particular type. In addition, we model controlling individual's speaking volume that can be effective to limit the virus spreading, and room ventilation.

- 1) Social distancing: We consider three kinds of risk scenarios regarding social distancing: high-, medium-, and low-risk scenarios. The relevant parameters that determine social distancing (defined in Table 1) are described with values in Table 3 as follows:
 - Physical distance D : If the distance between two agents is smaller than the sum of their radii then they overlap; such overlap indicates a contact between individuals, which may include hand-shaking, sneezing, kissing, etc.
 - Duration of contact T : We keep track of how long a susceptible agent stays in contact with an infected agent. The probability of transmission obviously increases for longer contact times.
 - Grouping G : Several agents can gather in a group and interact in it.²⁹ The size of a group is tunable, and the group may be either stationary or moving.
- 2) Self-isolation: It is a widely used protective measure—persons exposed to COVID-19 isolate themselves for some time in order to find out if they have become infectious.³⁰ Isolated agents in our model do not spread infection as they are modeled as having no infectious radius during isolation.

We define the self-isolation rate of infected agents as a user-defined percentage q_{percent} (Table 1) of infected agents that are isolated on a daily basis. The start time of isolation is defined by the corresponding parameter in Table 1.

- 3) Wearing face masks M : In certain situations, especially in close quarters and when a distance of at least 1.5 meters from others cannot be safely

maintained, individuals should wear a mouth-nose cover or a surgical mask.

In our model, we set three options for wearing masks with empirically estimated corresponding protection values. First, agents can wear FFP2 masks with a protection percentage of at least 94%³¹; we denote this by the protection value 3. Second, agents may choose to wear surgical masks with a protection percentage of at least 74%,³² which is denoted by the protection value 2. Finally, agents may choose not to wear masks; in this case the protection percentage is 0%, and this is denoted by the protection value 1.

- 4) Controlling one’s speaking volume V : We set five levels of volume when an infected agent speaks to a susceptible agent: silence has a value of 2, whispering a value of 3, talking a value of 4, speaking loudly a value of 5, and yelling has a value of 6. We choose these values to express how the speaking volume can affect the infectious radius. For example, based on Equation (1), if an infected agent with a radius of $r_i = 0.2$ m is yelling ($V = 6$) and does not wear a mask ($M = 1$), the infectious radius increases to a value of $r_{i,t+1} = 6.2$ m, which is an average value for traveling small particles with viral content in indoor environments as reported in Setti et al.³³
- 5) Room ventilation: We model the ability to ventilate a room by allowing the user to open/close the room’s door interactively during simulation time—we discuss this in detail in the next section.

Figure 3 shows an UML class diagram of our infection transmission model, where a particular Simulation scenario always contains:

- A particular locomotion model (in our simulations we use OSM as the main model). The MainModel class has a list of sub-models (e.g., CentriodGroupModel is an OSM sub-model managing the locomotion of groups of agents).
- A list of behaviors (e.g., Infection behavior). We implement class InfectionBehavior for the agents of PedestrianBehavior; method apply(List < Pedestrians >) changes the status of some agents from susceptible to infected and from infected to recovered. This change is done by method Model.update() without affecting the agents’ locomotion.
- A Topography that contains one Pedestrian (agent) or more. Each agent has its own InfectionHistory, a status (e.g., susceptible, infected, or recovered), and Pedestrian ProtectiveMeasures such as MaskType and PedestrianSpeakingVolume.

4. Interactivity of simulation

We aim at substantially enhancing the level of interactivity in the simulation process of infection transmission. Our interactive simulation approach offers the following advantages: (a) the user can actively modify the parameter values and characteristics of the VE (e.g., buildings and

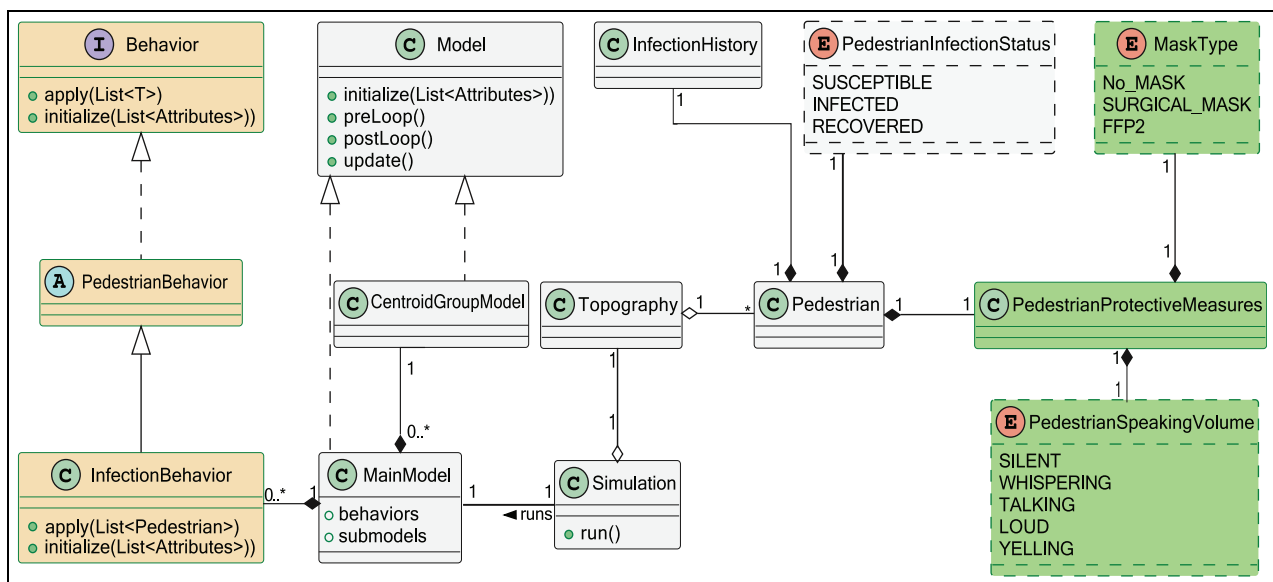


Figure 3. Infection transmission model: UML class diagram.

rooms) during the simulation; and (b) the user can examine the outcomes of the experiments in real time, and can interactively re-formulate and re-simulate scenarios of interest. This enables the user to interact with the simulation environment in real time in order to explore alternative strategies in the simulation process.

4.1. Modeling interactive door elements

In our simulation system built as an extended version of the Vadere framework, we design a new interactive door element: the user can change the state of a door from closed to open and vice versa during the simulation run time by a mouse double-click, thus affecting the behavior of agents.

Opening and closing a door allows air to flow between the rooms separated by that door.^{3,34,35} According to experts' opinion, opening and closing a door for a few minutes every hour provides a minimal level of room ventilation. In our model, this ventilation reduces the infection radius of the infected individual by a ventilation factor. The ventilation factor's value is inversely proportional to the ventilation duration and ranges from 0.1 to 1. For example, if the infection radius is 5 m prior to room ventilation, then after 10 min of ventilation the infection radius is multiplied by 0.1 to become 0.5 m.

In addition to ventilation, opening a closed door allows the agents to exit to a specific target outside. This reduces the current occupancy of a room, and, as a result, this also reduces the probability of an agent becoming infected.

Figure 4(a) shows an example of a simple topography consisting of two rooms separated by a wall with two interactive doors. Agents are created at sources S1 and S2 in the left room and they move to the target T in the right room through doors D1 and D2. Agents navigate to the target through the nearest open door. For example, agents created in S1 pass through D1 to the target, because D1 is closer to them than D2.

The figure illustrates different combinations of the doors' states and their effect on agents' trajectories:

- Figure 4(a): D1 and D2 are open.
- Figure 4(b): D1 is open, while D2 is closed interactively.
- Figure 4(c): D2 is open, while D1 is closed interactively.
- Figure 4(d): D2 is open, while D1 is closed interactively as in Figure 4(c); the difference to the previous scenario is that D1 is closed after two agents have already passed through it, so the other agents have to change their paths to the nearest open door.

The whole topography configuration is specified using the standard open format JSON. Listing 3 illustrates how doors are specified as JSON code, with the following attributes:

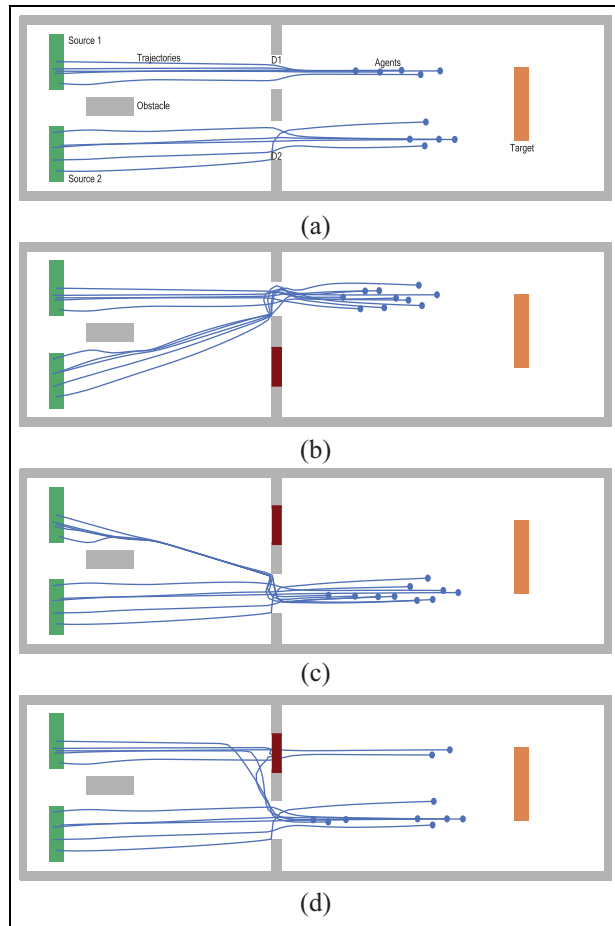


Figure 4. Opening and closing interactive doors by the user: (a) the two doors D1 and D2 are open, (b) D1 is open, and D2 is closed, (c) D1 is closed, and D2 is open, and (d) D1 is closed after two agents have passed through it; D2 is open.

Listing 3. JSON representation of an interactive door.

```

``doors`` : {
  ``shape`` : {
    ``x`` : 18,
    ``y`` : 2,
    ``width`` : 1.0,
    ``height`` : 1.5,
    ``type`` : ``RECTANGLE`` },
  ``id`` : 1,
  ``state`` : ``CLOSED`` , }

```

position (x , y), geometrical dimensions (width, height), geometrical shape (type), identification number (id), and current state (state).

4.2. Interactive change of agent's state

In our simulation system, we add a new capability that allows the user to change the state of any selected agent

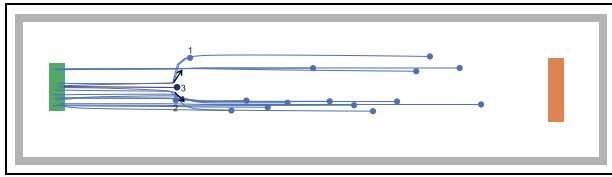


Figure 5. Agent 3 is stopped interactively by the user.

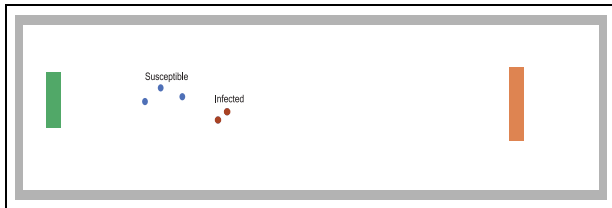


Figure 6. The user changes the status of two agents to infected.

from moving to non-moving by clicking the mouse. This allows the user to simulate agents in both situations, stopping and moving, like in real life.

Figure 5 shows an example with agent 3 who is stopped by the user during the simulation (by a mouse click); after that, because the stopped agent is located in the paths of agents 1 and 2, these agents try to avoid agent 3 as an obstacle. The black arrows represent the deviation of agent 1 and 2's trajectories. We also add a new feature that allows the user, by a mouse double-click on a selected agent, to change that agent's status from susceptible to infected and vice versa. Thus, the user can dynamically redistribute the infected agents to the desired locations.

Figure 6 shows another example: two agents for whom the user changes their status from susceptible to infected by mouse-click, while the other three agents remain susceptible.

Figure 7 shows the UML interaction diagram that represents user interactions with the VE.

The user can interrupt an element (e.g., a door) in the topography visualizer to change the state of that element. Our new interactive element manager module periodically checks whether the element is interactive (i.e., its state may or may not be changed). If it is interactive, the update notification is sent to the element in the VE.

While the locomotion OSM regularly updates all agents' next step positions, agents have to know the current state of doors, the locations of other agents (both moving and standing), and obstacles. For that, OSM must check the state of the interactive elements in the VE in order to avoid possible collisions. After the user has changed the environment interactively, we can estimate the probability of infection transmission, as illustrated by the experiments in the next section.

5. Experimental evaluation

We evaluate our simulation approach using the following two kinds of scenarios:

- Large-scale scenarios: study the spread of COVID-19 among 300,000 inhabitants in the city of Münster. At the scenarios' end, we aim to obtain the effective reproduction number $R_0^{eff}(t)$ and the pandemic curve.
- Small-scale scenarios: estimate the probability of infection transmission among at most 50 people in

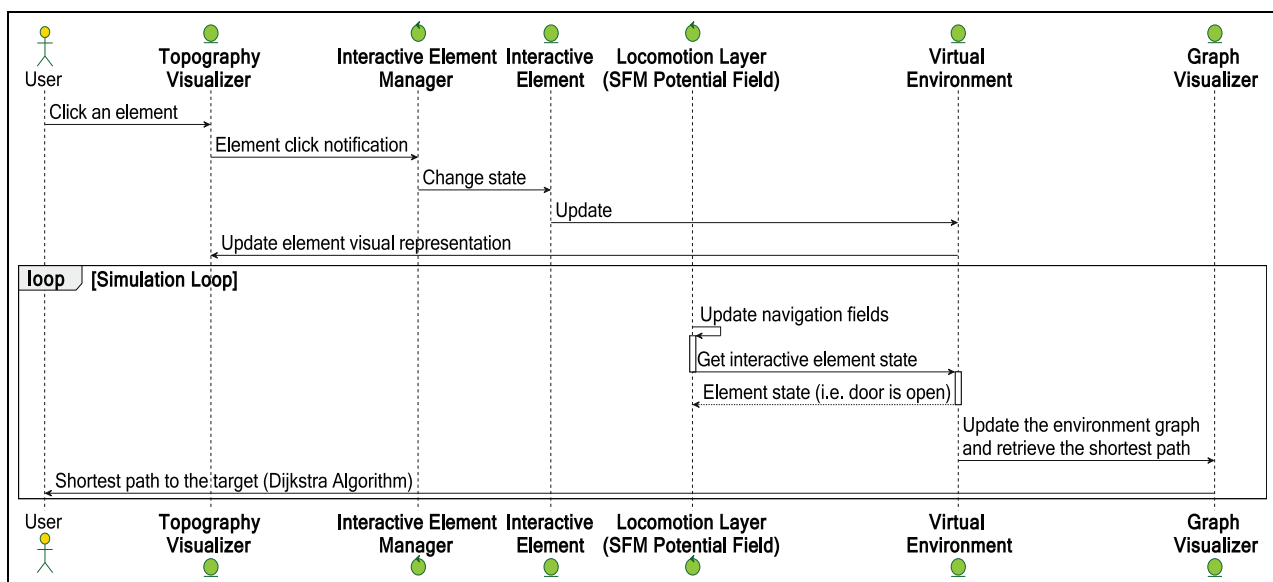


Figure 7. UML sequence diagram representing user's interactions with the simulation environment.

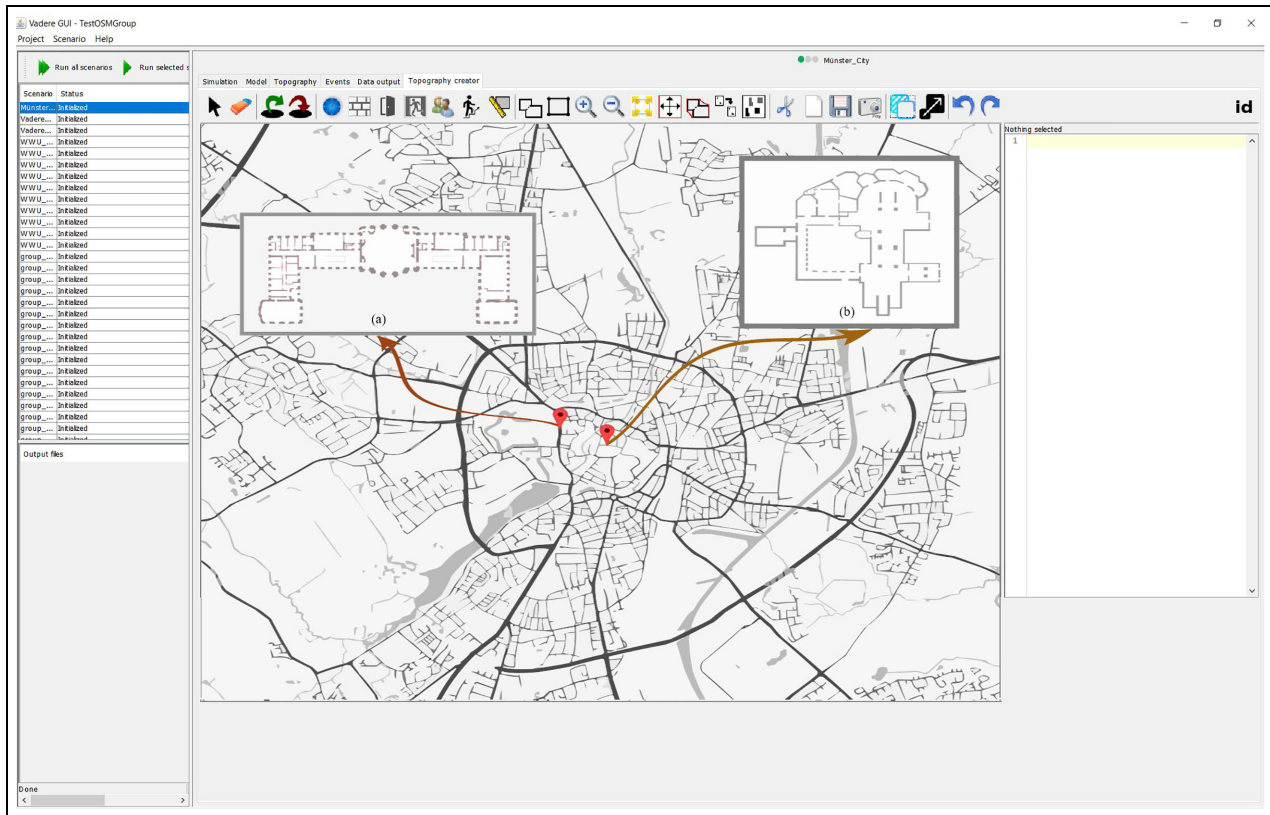


Figure 8. Geographic map of the city of Münster, with two particular buildings (a) and (b).

the common kinds of indoor environments. For each scenario, we aim at obtaining the probability that at least one individual will be infected.

Our simulations based on the model and implementation described above are performed on a computer with a CPU Ryzen Threadripper 2970 WX, 24 cores/48 threads, and 128 GB of memory. On this computer, it takes approximately 4 h to simulate the large-scale spread of the COVID-19 pandemic for 30 days using the time step of 2 min. We run small-scale scenarios on the same computer as large-scale scenarios. It takes about an hour to simulate a small-scale scenario of 4 h duration.

5.1. Time steps of simulation

To simulate large- and small-scale scenarios with different time resolution levels, we change the values of the simulation step, simulation time, and the ratio of real-time to simulation-time parameters in our simulation system. We define the virtual time in our simulations at two resolution levels:

- 1) In the 40 large-scale scenarios, the assumed duration of one time step is 2 min, which is the

minimum duration of contact in low-risk scenarios as specified in Table 3.

- 2) In the 60 small-scale scenarios, we decrease the duration of the time step to one second. One minute of loud speaking without wearing a mask can generate thousands of oral droplets per second, which can remain airborne for more than 8 min.³⁶ As a result, these droplets are more likely to be inhaled by individuals, resulting in new infections. In order to precisely monitor the changes in the probability of infection transmission along simulation time, we define the duration of one time step as 1 s.

5.2. Simulation scenarios

We create our simulation scenarios as follows:

- 1) Large-scale scenarios of COVID-19 are built for the city of Münster in Germany. For setting parameter values and for the model validation, we use the reported data provided by the European Green Capitals³⁷ and the official city website.³⁸

Figure 8 shows the geographic map of the city of Münster in the topography creator of our simulation system. The figure also shows the plans of two particular buildings in

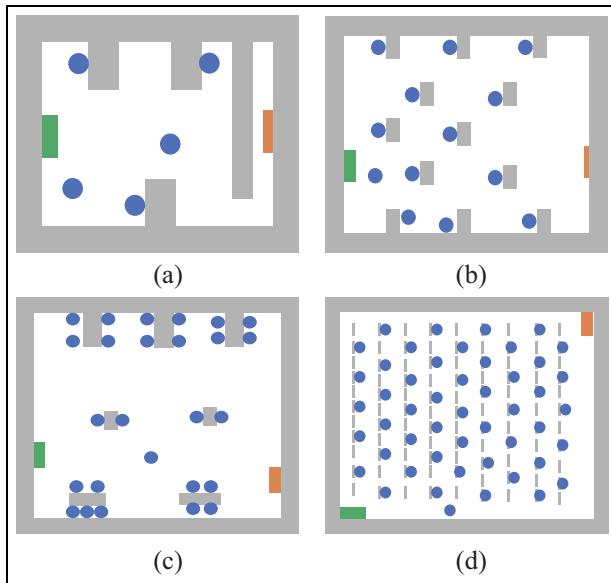


Figure 9. Examples: four kinds of simulation environments: (a) office, (b) classroom, (c) restaurant, and (d) hall.

the city: (a) the “castle” which is the administrative building of the University of Münster, and (b) the St. Paulus cathedral.

We simulate the real-life scenario: the city inhabitants perform a wide variety of daily activities while walking or sitting in different indoor environments. Daily activities include attending classroom lessons, working, shopping, or remaining isolated in homes or hospitals after they have become infected.

While moving from their source areas to their destination areas, agents may pass through target changer elements which redirect them to other intermediate targets inside the simulated VE. This ensures that agents are moving for the specified amount of time per day, after which the target changer elements redirect them to their final destinations (exit doors).

In this paper, we focus on agent behavior in indoor environments, rather than on large-scale movements as usually considered in frameworks based on GIS (Geographic Information Systems). In particular, we do not include trip patterns for agents in our scenarios, such as moving from one environment to another environment via transportation or other methods of travel (e.g., buses, cars, and trains).

Our simulation should evaluate if and how particular VEs prevent or facilitate the transmission of virus. We simulate the behavior of the whole 300,000 population of Münster³⁸ in different VEs, including: 19 schools with altogether 57,000 pupils, 20–30 pupils per classroom, the University of Münster with 45,000 students, 16 worship places with 200 to 400 people per church, 50 working

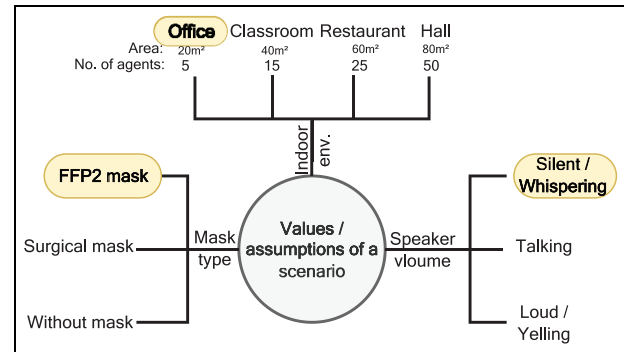


Figure 10. Example: parameters for a simulation scenario.

places with altogether 159,000 employees, and 15 central places such as malls, with 500 to 1500 people per place. Each of these VEs includes several rooms with connecting doors and corridors.

According to our model described above, we distinguish three classes in the city population: susceptible, infected, and removed, which change with time. Susceptible agents may become infected; removed agents either have recovered, are isolated, or died because of the virus.

- 2) Small-scale scenarios are studied in common indoor VEs: we estimate the probability of infection transmission from an infected individual to susceptible individuals in the most common VEs. This probability is affected by individuals’ movements in the VE, their activities with each other, and room ventilation.

Figure 9(a)–(d) show the layout of four typical example VEs with customized activities and duration of contacts, as follows:

- Figure 9(a): an office VE, with three employees working at desks for 4 h and two individuals moving.
- Figure 9(b): a classroom VE, with 12 students at their desks, interacting with a teacher in an 1-h lesson.
- Figure 9(c): a restaurant VE in which every family sits at a separate dinner table. In our experiments, the number of members of the family is assumed to vary from two to five; they stay for approximately 1–2 h for dinner.
- Figure 9(d): a concert hall VE, with 44 people attending a concert with three additional individuals as performers. The duration of the concert is 2 h.

Figure 10 shows an example of how our newly implemented options in the extended Vadere framework (choosing

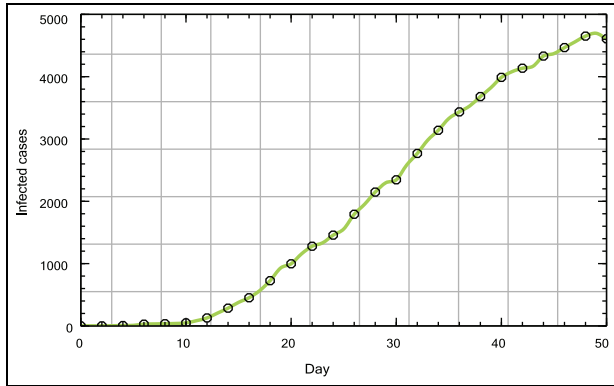


Figure 11. Daily infection numbers in Münster, March 1 to April 19, 2020.

the type of mask and adjusting the volume of the speaker) are used for creating and simulating a particular scenario: an office with five employees who work silently and wear FFP2 masks.

To study infection transmission in a broad variety of common environments, we run 60 different scenarios with various intervention options. In these scenarios, we study different situations with VE ventilation, which is performed by opening/closing doors regularly and with agents' speaking volumes ranging from silence to yelling. We report the results of these experiments in Section 5.4.2.

5.3. Simulation parameters

As important examples of simulation parameters, we discuss here the infection rate λ , basic reproduction number R_0 , effective reproduction number $R_0^{\text{eff}}(t)$, average duration of infection transmission τ , and probability of infection transmission $PR(t)$, as follows:

- 1) *Infection rate* λ : Figure 11 plots the daily numbers of infections in Münster after the first reported case (March 1, 2020) till day 50 (April 19, 2020) based on actual reported data taken from.³⁹

We utilize the logarithmic scale for expressing the rate of growth for non-linear functions, with the infection rate λ as example.⁴⁰ The natural logarithmic scale is preferred, as a model's parameters can then be interpreted as approximate proportional differences. For example, for rate $\lambda = 0.4$, a difference of 1 in the x -axis corresponds to a difference $\approx 40\%$ in the y -axis.⁴¹

Figure 12 depicts our estimate of the infection rate λ that utilizes the natural logarithm scale of the cumulative numbers of infected cases on the y -axis. We observe that the rate changes after day 20; we use the least-squares fitting method to observe the initial growth phase (from day 0 to 20), and we use the observed value to initialize our simulation model. As a result, the fitted line increases by

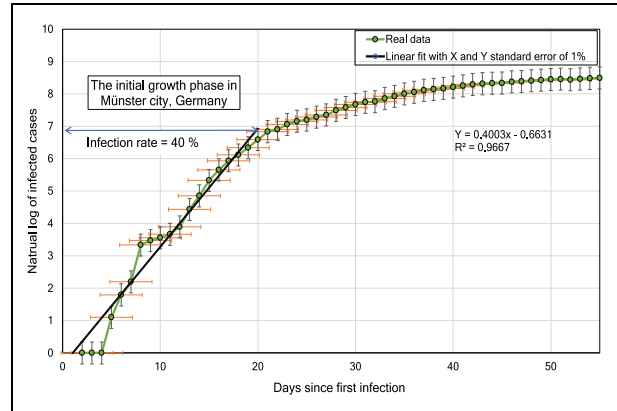


Figure 12. Natural logarithmic curve fitting to estimate the infection rate for Münster, Germany.

one step in the y -axis every 2.5 days (the x -axis is in days), or about $1/2.5$ per day; that is, the infection rate is 0.4 per day (40%). So, we can estimate the slope value using Microsoft Excel as follows:

$$y = 0.4003x - 0.6631, \quad (2)$$

where the coefficient of x indicates the infection rate.

We estimate the accuracy of fitting by using the determination coefficient R^2 from statistics, where the value of 1.0 indicates a perfect fit; our estimate calculated using Excel is $R^2 = 0.96$.

- 2) *Basic reproduction number* R_0 : we initialize the critical parameter R_0 which is the average number of people who obtain infection from an infectious individual: the larger the R_0 , the higher is the contagion level. For example, $R_0 = 5$ means that each infectious individual transmits infection to five persons on average. If $R_0 > 1$ then the infection level is increasing, otherwise decreasing. The value of R_0 is affected by both the environment and the acceptance level of protection measures by the population.⁴²

We initialize the value of the basic reproduction number R_0 based on the estimation proposed in paper⁴³ as follows:

$$R_0 = 1 + \lambda P, \quad (3)$$

where P is the average time in which a person can infect others, and λ is the rate of infection. As the estimation for P may not include isolation or hospitalization period, estimates of this time may differ, usually between 2 and 14 days.^{44,45}

In order to estimate the value of R_0 to be used as an initial value in our simulations, we take $P = 5$ days (which is a tunable parameter) as an assumed value in our simulations. Additionally, we use the infection rate $\lambda = 0.4$,

which was the infection rate during the first 20 days in Münster (estimated in Figure 12). Thus, using Equation (3), we calculate the value $R_0 = 3$ for the pandemic development in Münster.

- 3) *Effective reproductive number $R_0^{\text{eff}}(t)$* : is computed at each time step t by simulating each infectious person and counting how many of them have infected others, and then computing how many of them will infect others altogether in a particular period of time. We then average to S_{ave} , and we compute the effective reproductive number $R_0^{\text{eff}}(t)$ as follows:

$$R_0^{\text{eff}}(t) = R_0 \cdot S_{\text{ave}}, \quad (4)$$

where R_0 is the basic reproduction number, and S_{ave} is the average number of agents infected by each infectious agent.

- 4) *The average duration of infection transmission τ* : we empirically choose three values for the input parameter of the infection transmission duration based on the simulated risk level: 15 min for low-risk scenarios, 10 min for medium-risk scenarios, and 5 min for high-risk scenarios. These values can be tuned to simulate infection transmission of other virus variants like, for example, Delta or Omicron mutations. For example, in low-risk scenarios, if a susceptible agent contacts an infected agent for an average of $T = 2$ min and maintains a distance of 2.1 to 3 meters from the infected agent while remaining within his infectious radius for $\tau = 15$ min, the probability of a susceptible agent becoming infected is high as expressed by Equations (5) and (6).
- 5) *Probability of infection transmission $PR(t)$* : this probability depends on the type of contact activity among people. We set three categories of parameters to describe the various kinds of activities among people as follows:
1. Individual parameters, such as the volume of speech and the type of mask that each person wears.
 2. Environmental parameters, such as the area where the individuals reside.
 3. Inter-relational parameters, such as social distance and the duration of contact time between individuals.

This classification helps to assess the *risk of contact*. For example, COVID-19 is a disease with high contact-contagiousness: even a single exposure to a coughing individual

who is infected with COVID-19 in an office without wearing a mask for a time of 30 min usually leads to infecting susceptible individuals.

We calculate the risk of infection transmission to a susceptible agent within the infection radius as follows:

$$R(t) = 1 - e^{(k/\tau)}, \quad (5)$$

where k is a constant parameter (in our experiments we empirically estimate it to be -1.6), and τ is the average duration time in minutes required to transmit the infection. For instance, if the susceptible individuals do not wear masks, the infected individual is talking, and the average continuous time required to transmit the infection is $\tau = 15$ min, then the resulting risk of contact is $R(t) \approx 0.10$.

Summarizing, we compute the probability $PR(t)$ of a susceptible individual becoming infected through an infected individual in a room as follows:

$$PR(t) = 1 - (1 - R(t))^{S \cdot H}, \quad (6)$$

where S is the number of susceptible individuals in a room, and H is the current history (in min) of each susceptible individual being within the infection radius. For example, if $R(t) \approx 0.10$, the number of susceptible individuals in the room $S = 5$, and one of them has a current history of being in the infectious radius of an infected agent for $H = 40$ min, then the probability of this susceptible individual becoming infected is $PR(t) \approx 99\%$.

5.4. Simulation results

In the following, we report our simulation results for the large-scale and small-scale scenarios.

5.4.1. Large-scale: COVID-19 scenarios in the city of Münster. Our experiments simulate the spread of virus in 40 large-scale scenarios, from the worst to the best, based on how well the protective measures are followed by the population. In the worst scenario, we assume that 90% of people do not accept social distancing, infected cases are not isolated, and schools are not closed. In the best scenario, 90% of people follow social distancing, 90% of infected persons are isolated, and schools are closed. At the end of each scenario (150 days after the first case of infection), we evaluate the effective reproduction number that indicates the pandemic spread. Those scenarios that lead to $R_0^{\text{eff}}(t) < 1$ can be viewed as recommended as they limit or reduce the infection spread in the population.

Table 4 shows the resulting $R_0^{\text{eff}}(t)$ for our scenarios. The first column represents the percentages of population following high-, medium-, and low-risk social distancing guidelines. In these scenarios, neither self-isolation nor school closure are applied.

Table 4. Resulting $R_0^{eff}(t)$ for scenarios with high-, medium-, and low-risk social distancing.

Social distancing (%)	$R_0^{eff}(t)$		
	High	Medium	Low
10	3.00	2.38	2.30
20	2.92	2.30	2.21
30	2.89	2.23	2.15
40	2.81	2.18	1.96
50	2.74	2.11	1.91
60	2.67	2.07	1.82
70	2.55	2.01	1.75
80	2.49	1.97	1.65
90	2.41	1.94	1.50

In order to provide pandemic curves for our simulation scenarios during simulation run time, we customize the XChart plotting library.⁴⁶ Because the curve reflects the

infection status at the time of simulation run, it is continuously in progress: every simulation step contributes to the curve, and at the end of the simulation we have a complete curve. The x -axis represents time, while the y -axis represents the cumulative number of infections.

Figure 13 presents the results of simulating the high-risk scenarios regarding social distancing for the city of Münster. The scenarios represent different percentages of the population following the social distancing guidelines (from 10% to 90%). In the high-risk social distancing scenario, the physical distance between people ranges from 0.5 m to 1 m for the average contact time of 15 min, and individuals are composed in groups of five members. We observe in Figure 13 that, 34 days after the first infection, approximately 37,680 people are infected when 90% of the population behave according to the social distancing rules.

Figure 14 shows our experimental results for the scenario of medium-risk distancing; the distance between

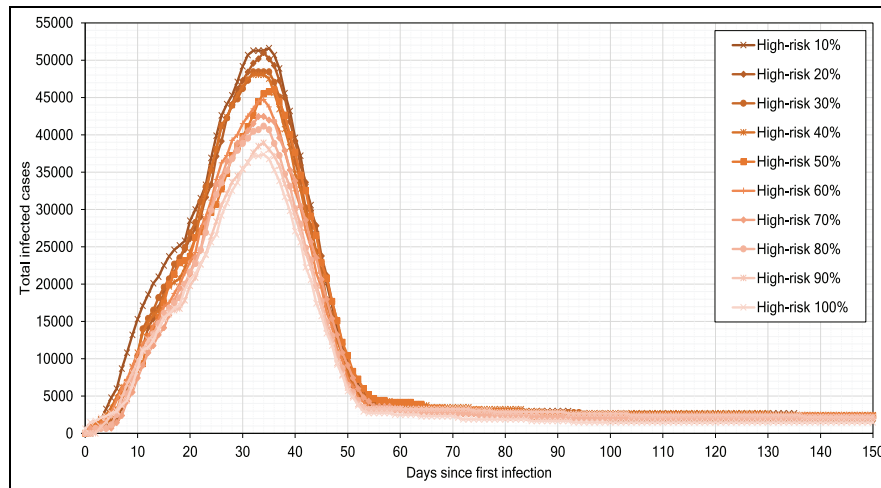


Figure 13. High-risk scenarios of pandemic development.

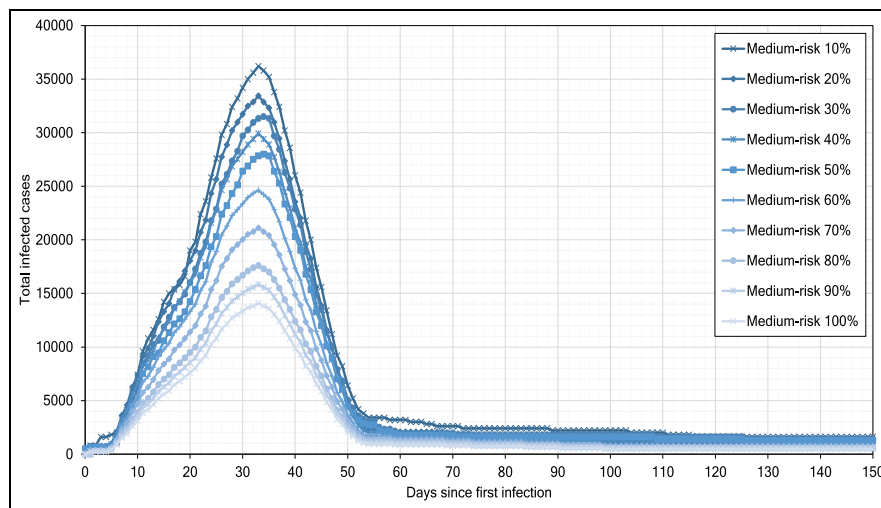


Figure 14. Medium-risk scenarios of pandemic development.

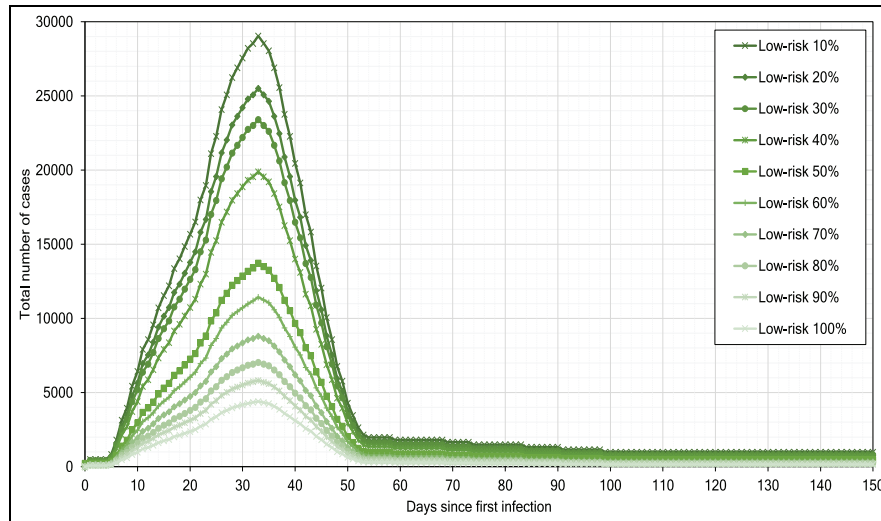


Figure 15. Low-risk scenarios of pandemic development.

Table 5. $R_0^{\text{eff}}(t)$ results of self-isolation scenarios.

Self-isolation (%)	$R_0^{\text{eff}}(t)$
10	2.26
20	2.13
30	2.04
40	1.99
50	1.93
60	1.82
70	1.71
80	1.69
90	1.66

individuals is between 1.1 m and 2 m for average contact time of 5 min while persons are in groups of three people. We observe that the infections number is decreasing to 16,094 on day 34 after the first infection if 90% of people follow the distancing rules.

Figure 15 depicts the outcomes of the low-risk scenarios, if the percentage of people following guidelines increases from 10% to 90%. We observe that if 90% of people participate in the measures for low risk then the infections number decreases to 5280 on day 34.

Our simulation experiments show that, although the low-risk scenarios help reduce the infections number, they alone cannot strongly delay or flatten the infection peak.

In our next experiment, we model scenarios with self-isolation of infected persons as a single measure, without social distancing and school closure, with the results presented in Table 5. The results show that the higher the percentage of isolated infected people, the lower the values of $R_0^{\text{eff}}(t)$ and, as a result, the lower the infection transmission.

Figure 16 presents the simulation results when self-isolation rules are followed by 10% to 90% of population.

We observe that self-isolation delays the peak of infection by 5–10 days for each 10% increase in the population fraction practicing self-isolation. On day 3 of infection (start of self-isolation = 3), agents are isolated for an average value period of 14 days until they recover (average duration of recovery $\gamma = 14$). We observe that self-isolation at 90% is quite helpful in reducing the peak to about 5320 people and flattening the pandemic curve. However, it alone does not suffice to stop the pandemic.

Table 6 summarizes combined best scenarios with self-isolation and low-risk distancing. We can see that combined protection measures and the highest degree of accepting them achieve together the best reduction in the infection rate and flattening the pandemic curve.

Figure 17 shows that self-isolation and low-risk distancing followed by 90% of people reduce the infection peak to 2100 cases.

In reality, schools in Münster were closed on day 43 after the first infection case.^{39,47} We experiment with school closing in three scenarios, where 0% indicates full attendance, 50% indicates that half of the students attend school in the morning shift, and 100% indicates full closure of schools; we compare our simulation results to the reported real-life curve for Münster in Figure 17. This comparison confirms that the reported curve for Münster is close to our simulation curve obtained for the 100% school closing scenario until day 58. After partial re-opening of schools on day 55, the infection number increases in the reported real-life curve, which is very near to our simulation curve for the scenario with 50% school closure.

Finally, we simulate the 0% school closure case and we forecast infections till day 150. We observe that school closure, self-isolation, and distancing together result in flattening the curve and strongly slow down the infection spread.

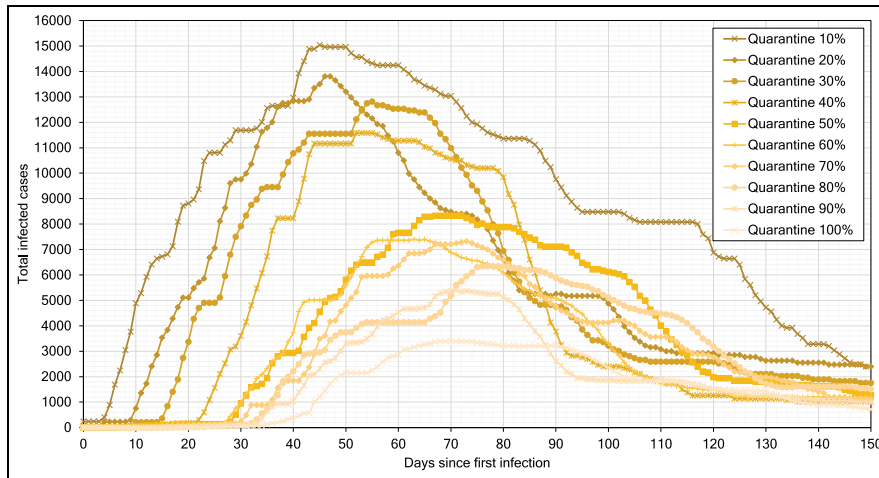


Figure 16. Effect of self-isolation from 10% to 90%.

Table 6. Results for combined self-isolation and low-risk.

Social distancing	Self-isolation (%)	School closures (%)	$R_0^{eff}(t)$
Low-risk			
90%	90	0	1.08
90%	90	50	0.91
90%	90	100	0.51

5.4.2. Small-scale: Indoor scenarios for COVID-19. As a result of simulating small-scale scenarios, we report the estimated probability of infection to at least one person present in one environment with an infected person.

Table 7 shows the probability $PR(t)$ of infection transmission when people use FFP2 masks. The changes in the

results are based on the change in the speaker’s volume (SV) – from silence to yelling – and the change in VEs. For instance, simulation shows that in a restaurant, when people are talking, the probability of at least one individual becoming infected after 100 min is 94%.

Table 8 shows how the probability of an individual becoming infected changes when people wear surgical masks.

Table 9 shows the probability of infection transmission when people do not wear masks.

One major way to reduce the probability of infection transmission is to increase room ventilation. The recommended airflow rate in indoor environments is 8–10 L/s per person in meeting rooms and classrooms.⁴⁸ We simulate room ventilation by interactively opening and closing room doors on a regular basis.

Figure 18(a)–(d) show the effect of ventilating the four kinds of VEs on the probability of infection transmission.

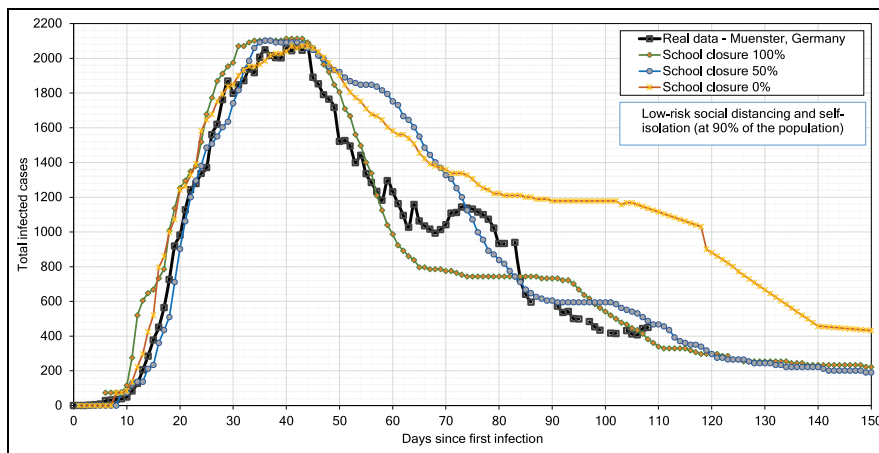


Figure 17. Effect of school closures.

Table 7. Probability estimations of infection transmission when individuals wear FFP2 masks.

Mask type: FFP2				
VE	SV	Infection time (m)	Infected no.	PR(t) (%)
Office	Silent	120	1	1
	Whispering	110	1	1
	Talking	90	1	60
	Loud	30	1	84
	Yelling	30	3	98
Classroom	Silent	120	1	1
	Whispering	110	1	1
	Talking	50	1	98
	Loud	30	1	98
	Yelling	30	3	98
Restaurant	Silent	120	1	84
	Whispering	110	1	90
	Talking	100	1	94
	Loud	50	1	96
	Yelling	40	7	97
Hall	Silent	100	1	10
	Whispering	50	7	99
	Talking	30	7	99
	Loud	30	10	99
	Yelling	30	17	99

Table 8. Probability estimations of infection transmission when individuals wear surgical masks.

Mask type: Surgical mask				
VE	SV	Infection time (m)	Infected no.	PR(t) (%)
Office	Silent	120	1	2
	Whispering	90	1	84
	Talking	70	1	98
	Loud	50	3	99
	Yelling	20	3	97
Classroom	Silent	120	1	1
	Whispering	100	1	1
	Talking	80	1	97
	Loud	60	3	97
	Yelling	30	3	98
Restaurant	Silent	100	1	94
	Whispering	60	1	94
	Talking	50	1	99
	Loud	30	3	99
	Yelling	30	5	99
Hall	Silent	100	1	50
	Whispering	80	6	98
	Talking	60	8	99
	Loud	40	18	98
	Yelling	30	18	99

We select one simulation run for each VE from Table 8 in which individuals wear surgical masks and speak with each other at the talking level. The risk of infection before

Table 9. Probability estimations of infection transmission when individuals do not wear masks.

Mask type: without masks				
VE	SV	Infection time (m)	Infected no.	PR(t) (%)
Office	Silent	40	3	96
	Whispering	45	4	94
	Talking	35	4	96
	Loud	30	4	99
	Yelling	20	4	99
Classroom	Silent	50	3	98
	Whispering	50	4	98
	Talking	30	8	98
	Loud	20	11	98
	Yelling	20	12	98
Restaurant	Silent	70	3	98
	Whispering	60	10	97
	Talking	40	19	94
	Loud	30	24	99
	Yelling	30	25	99
Hall	Silent	70	17	98
	Whispering	50	29	98
	Talking	30	44	98
	Loud	30	49	98
	Yelling	20	49	99

ventilation ranges from 97% to 99%, as shown in Table 8. Yet, after ventilation, the probability drops to a range of 0% to 6.5%, as shown in: Figure 18(a) for the office VE, Figure 18(b) for the classroom VE, Figure 18(c) for the restaurant VE, and Figure 18(d) for the hall VE.

5.5. Limitations of our approach

Our simulation model and its current implementation have a number of limitations. First, currently we model only three possible health states for agents, namely: susceptible, infected, and recovered. We do not consider other possible states, for example exposed and hospitalized. Second, we assume that infection transmission does not occur in open air but only in buildings and rooms. Additionally, we do not model agents' trips in the outdoors, such as moving from home to work and back home, and we do not include transportation and traveling in our consideration. Because of this restriction, our simulation model would be not suitable for other kinds of pandemics that are developed primarily due to the infection transmission in open air. Fourth, our scenarios do not simulate multiple virus mutations with different infection rates simultaneously.

A further restriction of our model is that we assume for simplicity that infection is only possible within the infectious radius of an infected individual. In reality, aerosols are divided into two types: large droplets that fall to the ground and surfaces based on the atmospheric conditions of the room, and small droplets that remain

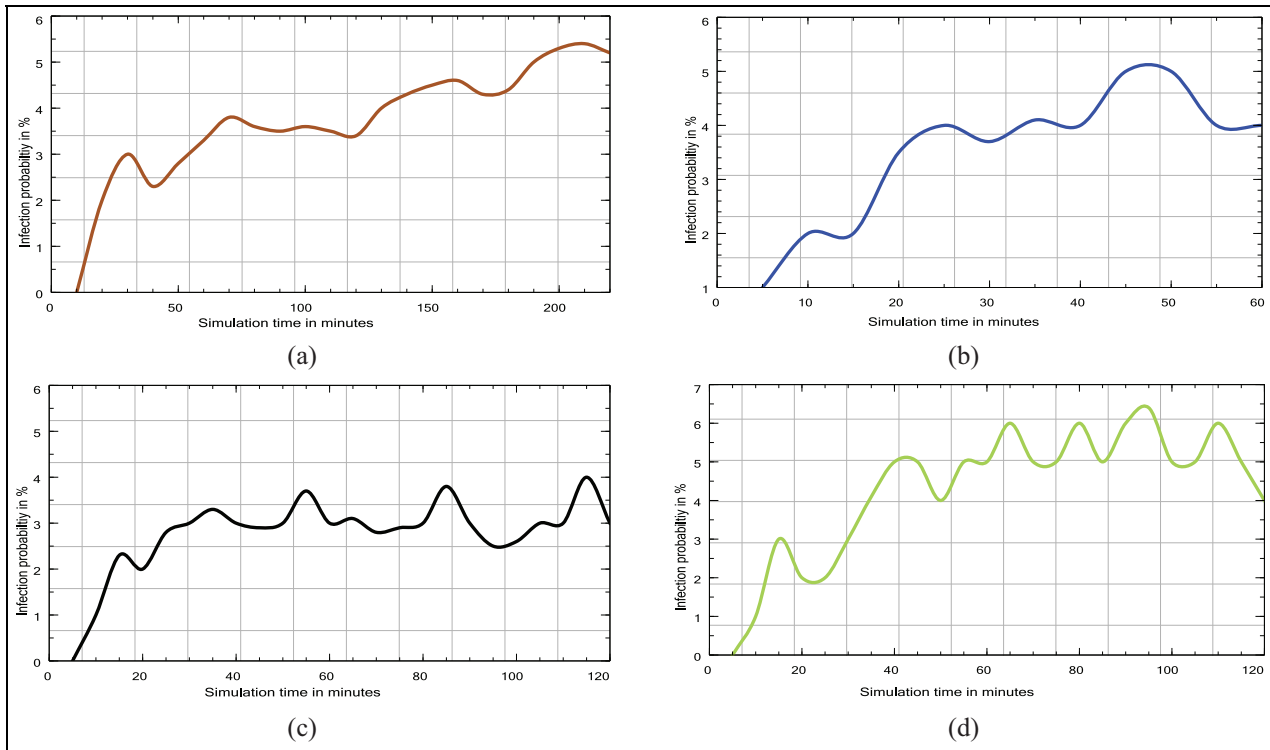


Figure 18. Four probability estimation plots for small-scale scenarios: (a) office, (b) classroom, (c) restaurant, and (d) hall.

suspended in the air for extended periods of time⁴⁹ and can move over longer distances. The primary mode of infection transmission is via breathing airborne droplets. Additionally, infection transmission through large droplets often happens by direct contact, such as shaking hands with an infected individual or touching the door handle and then rubbing eyes.⁵⁰ These droplets are thought to spread widely with varying densities and pose a risk to everyone in a small or moderately sized indoor room. Therefore, it is possible that the transmitted airborne particles will spread in areas beyond our calculated infection radius, thus additionally affecting the number of infected individuals.

In future work, we plan to address the restrictions and weaknesses of our modeling and simulation approach.

6. Conclusion

In this paper, we introduce and implement a novel model of infection/virus transmission in the SIR format, and we apply it to simulate the recent COVID-19 pandemic. We develop a new concept of behaviors based on pedestrian dynamics and we implement it by extending the existing Vadere simulation framework. In our simulation system, we greatly enhance the Vadere's level of user interactivity in the process of simulation. This allows the user to control by mouse-clicks the state of the agents (stationary/moving

and susceptible/infected) and to add new interactive elements, for example, doors that can be opened/closed interactively during simulation.

We evaluate our approach in a series of extensive simulation experiments for the city of Münster in Germany, which has a population of approximately 300,000 people. We conduct simulation experiments for high-, medium-, and low-risk distancing scenarios, together with school closure and self-isolation. Our experimental results show that early social distancing, self-isolation and school closures are keys to fighting the COVID-19 pandemic and that individual behavior, like following rules/regulations, is essential in controlling the spread of infection. We also show that no single protective measure can significantly prevent infection, but rather a combination of several measures should be applied. We further model and simulate the infection behavior and assess the efficacy of wearing masks and controlling speaking volume in most common indoor VEs (classroom, office, hall, and restaurant). By comparing our numerous simulation results with the real-life reported pandemic data for both city of Münster and indoor environments, we confirm the adequacy of our modeling and simulation approach.


Acknowledgements

Thanks to Dr. Celeste Brenneka (University of Münster) for proofreading the article.

Funding

Mina Abadeer was supported by a scholarship from Christian Vision UK. Sergei Gorlatch is supported by the DFG project PPP-DL at the University of Münster.

ORCID iD

Mina Abadeer  <https://orcid.org/0000-0002-1088-3228>

References

- Bichara D, Kang Y, Castillo-Chavez C, et al. SIS and SIR epidemic models under virtual dispersal. *Bull Math Biol* 2015; 77(11): 2004–2034.
- Bertozzi AL, Franco E, Mohler G, et al. The challenges of modeling and forecasting the spread of COVID-19. *Proc Natl Acad Sci* 2020; 117(29): 16732–16738.
- Morawska L, Tang JW, Bahnfleth W, et al. How can airborne transmission of COVID-19 indoors be minimised? *Environ Int* 2020; 142: 105832.
- Getz WM, Carlson C, Dougherty E, et al. An agent-based model of school closing in under-vaccinated communities during measles outbreaks. *Simulation* 2019; 95(5): 385–393.
- Kleinmeier B, Zönnchen B, Gödel M, et al. Vadere: an open-source simulation framework to promote interdisciplinary understanding. *arXiv preprint arXiv:190709520* 2019.
- Funk S, Salathé M and Jansen VAA. Modelling the influence of human behaviour on the spread of infectious diseases: a review. *J R Soc Interface* 2010; 7(50): 1247–1256.
- Du E, Chen E, Liu J, et al. How do social media and individual behaviors affect epidemic transmission and control? *Sci Total Environ* 2021; 761: 144114.
- Rath B, Gao W and Srivastava J. Evaluating vulnerability to fake news in social networks: a community health assessment model. In: *2019 IEEE/ACM international conference on advances in social networks analysis and mining (ASONAM)*, 2019, pp.432–435. Canada: IEEE
- Brainard J and Hunter PR. Misinformation making a disease outbreak worse: outcomes compared for influenza, monkeypox, and norovirus. *Simulation* 2020; 96(4): 365–374.
- Wells WF. Airborne contagion and air hygiene. an ecological study of droplet infections. *JAMA* 1955; 159(1): 90.
- Riley EC, Murphy G and Riley RL. Airborne spread of measles in a suburban elementary school. *Am J Epidemiol* 1978; 107(5): 421–432.
- Yates TA, Khan PY, Knight GM, et al. The transmission of Mycobacterium tuberculosis in high burden settings. *Lancet Infect Dis* 2016; 16(2): 227–238.
- Noakes CJ, Beggs CB, Sleigh PA, et al. Modelling the transmission of airborne infections in enclosed spaces. *Epidemiol Infect* 2006; 134(5): 1082–1091.
- Furuya H. Risk of transmission of airborne infection during train commute based on mathematical model. *Environ Health Prev Med* 2007; 12(2): 78–83.
- Chen S, Chang C and Liao C. Predictive models of control strategies involved in containing indoor airborne infections. *Indoor Air* 2006; 16(6): 469–481.
- Guo Y, Qian H, Sun Z, et al. Assessing and controlling infection risk with wells-riley model and spatial flow impact factor (SFIF). *Sustain Cities Soc* 2021; 67: 102719.
- Sun C and Zhai Z. The efficacy of social distance and ventilation effectiveness in preventing COVID-19 transmission. *Sustain Cities Soc* 2020; 62: 102390.
- Vardavas R, de Lima PN and Baker L. Modeling COVID-19 nonpharmaceutical interventions: exploring periodic NPI strategies. *medRxiv*. Epub ahead of print 21 March 2021. DOI: 10.1101/2021.02.28.21252642.
- Cockrell C, Ozik J, Collier N, et al. Nested active learning for efficient model contextualization and parameterization: pathway to generating simulated populations using multi-scale computational models. *Simulation* 2021; 97(4): 287–296.
- Altamimi T, Khalil H, Rajus VS, et al. Cell-DEVS models with BIM integration for airborne transmission of COVID-19 indoors. In: *Proceedings of the 2021 symposium on simulation for architecture and Urban design*, Canada, 2021.
- Ayadi A, Frydman C, Laddada W, et al. Combining Devs and semantic technologies for modeling the SARS-CoV-2 replication machinery. In: *2021 Annual Modeling and Simulation Conference (ANNSIM), USA, 2021*, pp.1–12.
- Gomez J, Prieto J, Leon E, et al. INFEKTA—an agent-based model for transmission of infectious diseases: the COVID-19 case in Bogotá, Colombia. *PLoS One* 2021; 16(2): e0245787.
- Chang SL, Harding N, Zachreson C, et al. Modelling transmission and control of the COVID-19 pandemic in australia. *Nat Commun* 2020; 11(1): 1–13.
- Hack JJ and Papka ME. The U.S. High-performance computing consortium in the fight against COVID-19. *Comput Sci Eng* 2020; 22(6): 75–80.
- MITRE's infectious disease analytics team. Stopping COVID-19: short-term actions for long-term impact. Technical report, MITRE, March 2020.
- Seitz MJ. *Simulating pedestrian dynamics*. PhD Thesis, Technische Universität München, 2016.
- Mayr CM and Köster G. Social distancing with the optimal steps model. *arXiv preprint arXiv:200701634* 2020.
- Pezoa F, Reutter JL, Suarez F, et al. Foundations of JSON schema. In: *Proceedings of the 25th international conference on world wide web*, Montréal, Québec, Canada, 2016, pp.263–273.
- Abadeer M and Gorlatch S. Distributed simulation of crowds with groups in crowdSim. In: *2019 IEEE/ACM 23rd international symposium on distributed simulation and real time applications (DS-RT)*, Italy, 2019, pp.1–8.
- Wamsley L and Simmons-Duffin S. The science behind a 14-day quarantine after possible COVID-19 exposure. Technical report, Health News From NPR, 2020.
- Li KKW, Jousseaume AM, Kwan JKC, et al. FFP3, FFP2, N95, surgical masks and respirators: what should we be wearing for ophthalmic surgery in the COVID-19 pandemic? *Graefes Arch Clin Exp Ophthalmol* 2020; 258(8): 1587–1589.
- Asadi S, Cappa CD, Barreda S, et al. Efficacy of masks and face coverings in controlling outward aerosol particle emission from expiratory activities. *Sci Rep* 2020; 10(1): 1–13.

33. Setti L, Passarini F, De Gennaro G, et al. Airborne transmission route of COVID-19: why 2 meters/6 feet of interpersonal distance could not be enough. *Int J Environ Res Public Health* 2020; 17(8): 2932.
34. Sansone E and Keimig S. The influence of door swing and door velocity on the effectiveness of directional airflow. *Proc ASHRAE IAQ* 1987; 87: 372–381.
35. Bazant MZ and Bush JWM. A guideline to limit indoor airborne transmission of COVID-19. *Proc Natl Acad Sci* 2021; 118(17): e2018995118.
36. Tang S, Mao Y, Jones RM, et al. Aerosol transmission of SARS-CoV-2? Evidence, prevention and control. *Environ Int* 2020; 144: 106039.
37. European Green Capital . *Muenster competes for the title "European Green Capital"*, http://www.muenster.de/stadt/greencapital/index_en.html (2020, accessed 2 April 2020).
38. Stein B, Hertel T and Borgers W. *Welcome to Muenster*, https://www.stadt-muenster.de/fileadmin/user_upload/stadt-muenster/en/pdf/welcome_to_ms.pdf (2020, accessed 2 April 2020).
39. *Coronavirus im Regierungsbezirk Münster*, https://www.bezreg-muenster.de/de/im_fokus/uebergreifende_themen/coronavirus/coronavirus_allgemein/index.html (2020, accessed 21 April 2020).
40. Scalia Tomba G, Vynnycky E and White RG. An introduction to infectious disease modelling. *Eur J Public Health* 2010; 22(2): 295–295.
41. Gelman A and Hill J. *Data analysis using regression and multilevel/hierarchical models*. Cambridge University Press, Cambridge, UK, 2006.
42. Dietz K. The estimation of the basic reproduction number for infectious diseases. *Stat Methods Med Res* 1993; 2(1): 23–41.
43. Jones JH. *Notes on R0*. California: Department of Anthropological Sciences, 2007, p. 323..
44. Böhmer MM, Buchholz U, Corman VM, et al. Investigation of a COVID-19 outbreak in Germany resulting from a single travel-associated primary case: a case series. *Lancet Infect Dis* 2020; 20(8): P920–P928.
45. Sanche S, Lin YT, Xu C, et al. Early release-high contagiousness and rapid spread of severe acute respiratory syndrome coronavirus 2. *Emerg Infect Dis* 2020; 26(7): 1470–1477.
46. *XChart*. *XChart*, 2020. <https://knowm.org/open-source/XChart/>, (accessed 30 May 2022)
47. *Coronavirus (in German): Erste Infektion in Münster*, <https://www.allesmuenster.de/coronavirus-erste-infektion-in-muenster/> (2020, accessed 30 May 2020).
48. Olesen BW. Indoor environmental input parameters for the design and assessment of energy performance of buildings. *REHVA J* 2015; 52: 17–23.
49. Morgenstern J. Aerosols, droplets, and airborne spread: Everything you could possibly want to know. *First10EM blog* 2020; 6.
50. Stadnytskyi V, Bax CE, Bax A, et al. The airborne lifetime of small speech droplets and their potential importance in SARSCoV-2 transmission. *Proc Natl Acad Sci* 2020; 117(22): 11875–11877.

Author biographies

Mina Abadeer is a PhD candidate at the University of Münster in Germany since 2018. He received his MSc in Computer Engineering from the Arab Academy for Science, Technology, and Maritime Transport in Egypt, and he worked as a Research Assistant at the American University in Cairo (Egypt). His research interests include emergency evacuation and epidemic simulation, computer networking, and cloud computing.

Sameh Magharious is a Computer Engineering (B.Sc.) Principal Engineer at Dell EMC (USA), where he focuses on designing and developing internet-scale cloud services. He was also a member of Microsoft's Office Core Engineering group, where he worked on storage infrastructure and sync/collaboration features for Office 365. His research focuses on computer simulation and distributed systems.

Sergei Gorlatch is Full Professor of Computer Science at the University of Münster (Germany) since 2003. Earlier he was Associate Professor at the Technical University of Berlin, Assistant Professor at the University of Passau, and Humboldt Research Fellow at the Technical University of Munich. Prof. Gorlatch has more than 200 peer-reviewed publications in renowned international journals and conferences. He holds MSc degree from Kiev Shevchenko University, PhD degree from Glushkov Institute of Cybernetics (Ukraine), and Habilitation degree from the University of Passau (Germany). His research interests include parallel and distributed programming, formal methods, and networking.